

Bulk antiferromagnetism in $\text{Na}_{0.82}\text{CoO}_2$ single crystals

S. Bayrakci¹, C. Bernhard¹, D. P. Chen¹, B. Keimer¹, R. K. Kremer¹,
P. Lemmens¹, C. T. Lin¹, C. Niedermayer², and J. Strempler¹

¹Max Planck Institute for Solid State Research, Heisenbergstr. 1, D-70569 Stuttgart, Germany

²Paul-Scherrer-Institut, CH-5232 Villigen, Switzerland

(Dated: May 22, 2019)

Susceptibility, specific heat, and muon spin rotation measurements on high-quality single crystals of $\text{Na}_{0.82}\text{CoO}_2$ have revealed bulk antiferromagnetism with Néel temperature $T_N = 19.8 \pm 0.1$ K and an ordered moment perpendicular to the CoO_2 layers. The magnetic order encompasses nearly 100% of the crystal volume. The susceptibility exhibits a broad peak around 30 K, characteristic of two-dimensional antiferromagnetic fluctuations. The in-plane resistivity is metallic at high temperatures and exhibits a minimum at T_N .

PACS numbers: 75.30.-m, 76.75.+i, 72.80.Ga, 71.30.+h

Long-standing interest in the interplay between spin, charge, and orbital degrees of freedom in cobalt oxides has increased following the recent discovery of superconductivity in the hydrated cobaltate $\text{Na}_{0.35}\text{CoO}_2 \cdot 1.3\text{H}_2\text{O}$ (Ref. 1). Its transition temperature, $T_c = 4.6$ K, is much lower than those of the layered copper oxides, but higher than that of Sr_2RuO_4 , the only other known layered transition metal oxide which exhibits superconductivity. The crystal structure of this compound contains distorted, edge-sharing CoO_6 octahedra such that the Co sites form a triangular lattice^{2,3}. The electronic structure is quasi-two-dimensional^{4,5,6,7}. Unconventional superconductivity has been proposed based on NMR experiments^{8,9} and model calculations^{4,10,11,12}, but many important questions about the symmetry of the order parameter and the character of the quasi-particles at the Fermi surface have yet to be answered.

The triangular CoO_2 layers of Na_xCoO_2 are isostructural to those of $\text{Na}_{0.35}\text{CoO}_2 \cdot 1.3\text{H}_2\text{O}$ (Refs. 13,14,15). It may therefore serve as a reference system with respect to the effects of doping and magnetic correlations. Na_xCoO_2 is metallic¹⁶ and exhibits an unusual Hall effect¹⁷, as well as a very large thermopower¹⁸. The thermopower increases with increasing x ¹⁹, which in a local-moment picture corresponds to a progressive dilution of magnetic Co^{4+} ($S = 1/2$) with nonmagnetic Co^{3+} ($S = 0$). Following observations of a pronounced field dependence, a magnetic mechanism has been invoked to explain the large thermopower¹⁷. It is therefore important to determine the magnetic ground state and exchange parameters in this material.

We have taken a first step in this direction by synthesizing high-quality single crystals of Na_xCoO_2 with $x \sim 0.8$ and studying their resistivity, specific heat, and magnetic susceptibility as a function of temperature. An antiferromagnetic state with Néel temperature $T_N = 19.8 \pm 0.1$ K and an ordered moment perpendicular to the CoO_2 layers was observed. Muon spin rotation (μSR) measurements confirm that the static magnetic order encompasses nearly 100% of the volume. The in-plane resis-

tivity shows a minimum around the magnetic phase transition. The susceptibility exhibits a broad peak around 30 K, characteristic of two-dimensional antiferromagnetic fluctuations. These findings may be indicative of a quasi-two-dimensional commensurate spin density wave.

Cylindrical single crystals of diameter 6 mm and length 80 mm were grown in an optical floating-zone furnace. The initial polycrystalline material was prepared using a mixture of Na_2CO_3 and Co_3O_4 with a Na:Co ratio of 0.8:1. The powders were calcined at 750 °C for 12 hours and then reacted at 850 °C for a day with intermediate grindings. The mixture was pressed to form a cylinder and premelted prior to growth. The molten zone was passed through the feed rod under oxygen flow at a rate of 2 mm/h. Details will be published elsewhere²⁰. Pieces cut from two of the resulting crystals were analyzed by inductively coupled plasma atomic emission spectroscopy and atomic absorption spectroscopy. The Na:Co ratios were found to be 0.82 ± 0.02 and 0.83 ± 0.02 , respectively. The virtually identical compositions attest to good reproducibility of the crystal preparation. The Néel temperatures of both samples were also identical within experimental error. Single-crystal and powder x-ray diffraction confirm a nearly pure phase with space group $P6_3/mmc$, in good agreement with Ref. 15 and with Raman scattering experiments²¹. The lattice parameters were determined by single-crystal x-ray diffraction along $(h, h, 0)$ and $(0, 0, l)$ at room temperature, resulting in values of $a = 2.843(1)\text{Å}$ and $c = 10.687(5)\text{Å}$. The susceptibility, specific heat, and resistivity measurements were carried out in Quantum Design MPMS and PPMS systems.

Fig. 1 shows the magnetic susceptibility measured in a 5T magnetic field oriented either along the c -axis or perpendicular to it. Upon cooling, the anisotropy increases, and a broad peak develops around 31 ± 3 K. This is indicative of short-range, Ising-type, quasi-two-dimensional antiferromagnetic correlations. A sharp decrease of the c -axis susceptibility around 20 K heralds an antiferromagnetic transition with ordered moments along c . The inset in Fig. 1 shows that the transition is sharp

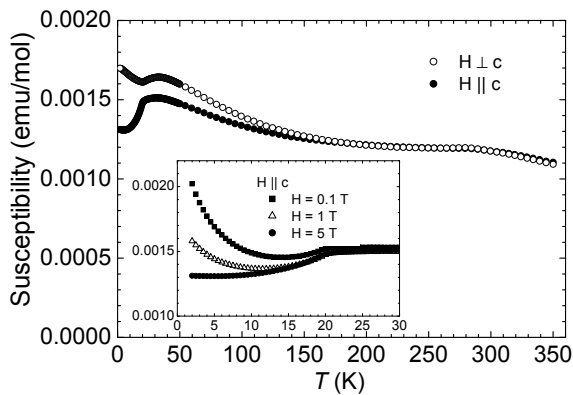


FIG. 1: Magnetic susceptibility of $\text{Na}_{0.82}\text{CoO}_2$ measured on cooling in a 5T magnetic field oriented along (open symbols) and perpendicular to (closed symbols) the c -axis. Inset: Low-temperature susceptibility along c in different applied fields.

and only weakly affected by the field. Curie tails, presumably due to paramagnetic impurities, are suppressed in a 5T field.

A broad hump in the susceptibility is evident at around $285 \pm 5\text{K}$, for all sample orientations and at all applied magnetic fields. This temperature corresponds roughly to the onset of the low-temperature splitting of a phonon mode at $\nu \sim 550\text{cm}^{-1}$, as observed in IR conductivity measurements (not shown). This suggests that this feature in the susceptibility arises from a structural phase transition intrinsic to $\text{Na}_{0.8}\text{CoO}_2$, rather than from an impurity phase such as CoO (an antiferromagnet with $T_N = 292\text{K}$). This interpretation is consistent with x-ray powder diffraction measurements, which exhibit no traces of CoO. The origin of the structural transition remains to be determined.

The specific heat, C_P , also exhibits a sharp anomaly at $19.8 \pm 0.1\text{K}$, which indicates the onset of long-range antiferromagnetic ordering (Fig. 2). The entropy contained in this anomaly amounts to $0.08(1)\text{J/molK}$ and corresponds to about 10% of the entropy of the Co^{4+} spin-1/2 system. There is a slight excess heat capacity above T_N , extending up to $\sim 35\text{K}$. These observations are consistent with the short-range magnetic fluctuations above T_N visible in the magnetic susceptibility measurements.

The specific heat at low temperatures contains a contribution linear in temperature which is revealed in a $C_P/T = \gamma + \beta T^2$ plot (inset in Fig. 2). It is slightly sample-dependent and amounts to $8.4(3)$ and $10.4(4)\text{mJ/molK}^2$ for the two measured crystals. We ascribe it to the Sommerfeld term from the conduction electrons. If the cubic term β is attributed to the contribution of acoustic phonons alone (ignoring possible contributions from magnons), it corresponds to a Debye temperature of $\sim 420\text{K}$.

Muon-spin-rotation (μSR) experiments have been performed using the GPS setup at the πm^3 beamline at

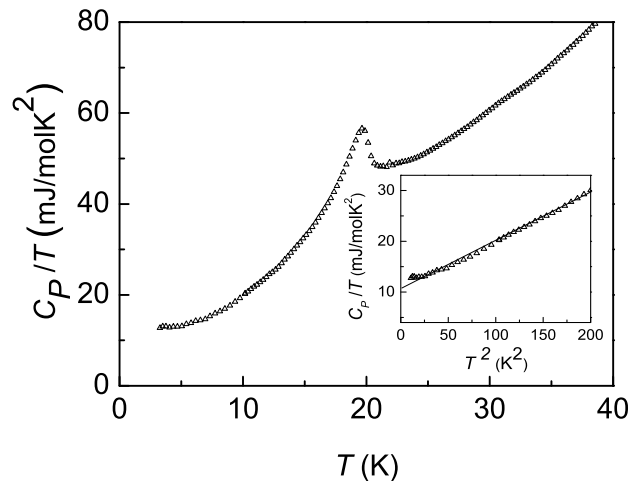


FIG. 2: Specific heat of a $\text{Na}_{0.82}\text{CoO}_2$ crystal. Inset: Low-temperature specific heat in a $C_P/T = \gamma + \beta T^2$ plot.

the Paul-Scherrer-Institute (PSI) in Villigen, Switzerland, which provides 100% spin-polarized muons. The μSR technique is especially suited for the investigation of magnetic materials with small magnetic moments. In particular, it allows one to study the homogeneity of the magnetic state on a microscopic scale, and also to access its volume fraction. The accessible time scale is 10^{-6} - 10^{-10}s . The muons are implanted into the bulk of the material, where they thermalize rapidly without any noticeable loss in their initial polarization. They stop at well-defined (but in general unknown) interstitial lattice sites. In the present compound, they most likely form a muoxyl bond with an oxygen atom in the CoO_2 planes or occupy empty Na sites in between the CoO layers. The whole ensemble of muons is randomly distributed throughout a layer with a thickness of about $200\mu\text{m}$, and thus probes a representative part of the sample volume. The muons decay (with a mean lifetime of $\tau_\mu = 2.2\mu\text{s}$) into two neutrinos and a positron which is preferentially emitted along the direction of the muon spin at the instant of decay. The time evolution of the spin polarization, $P(t)$, of the muon ensemble can thus be obtained via the time-resolved detection of the spatial asymmetry of the positron emission rate.

Fig. 3a shows μSR spectra obtained at $T=7.5\text{K}$ in a zero-field configuration. The normalization of the total asymmetry of the polarization function is based on the measurement in a weak transverse field of 100 Oe at 50 K, where the sample is in the paramagnetic state. Spectra for two different orientations of the muon spin-polarization with respect to the crystallographic c -axis are shown. It is evident that the spectra contain several oscillating components, which means that the muons experience several well-defined local magnetic fields. Even without any further analysis, one can immediately conclude that a large fraction of the sample volume must exhibit static magnetic order. We analyzed the spectra

using a relaxation function of the form

$$P(t) = P(0) \sum_i A_i \cos(2\pi\nu_\mu^i t) \exp(-\lambda^i t). \quad (1)$$

An excellent description of the data can be obtained with a sum of three oscillatory terms with frequencies and relaxation rates (at low temperature) $\nu_\mu = 1.25, 2.6$ and 3.2 MHz and $\lambda = 0.8, 1.2$ and $2.8 \mu\text{s}^{-1}$, plus one non-oscillatory term with a very small relaxation rate of $\lambda = 0.02 \mu\text{s}^{-1}$ that accounts for the component of the muon spin parallel to the internal fields (lines in Fig. 3a). The frequencies of the oscillating components do not depend on the direction of the muon spin, while their amplitudes, A_i , exhibit a strong variation. The amplitudes for the different muon-spin orientations can be used to determine the direction of the local magnetic fields, as well as the corresponding magnetic volume fractions. The spectra suggest that the muons experience three different well-defined local magnetic fields which point in different directions. The highest field is parallel to the c -axis (within the error bar) and amounts to about 17% of the entire signal. The 2.6 MHz signal is at an angle of about 25° with respect to the c -axis and comprises nearly 33% of the total amplitude. Finally, the 1.2 MHz signal is at an angle of 43° and represents about 50% of the entire signal. Based on this analysis, we thus find that the volume fraction of the magnetic state is in excess of 95%: that is, the entire sample is magnetically ordered within the error of our measurement.

Evidence for antiferromagnetic ordering in Na_xCoO_2 was also obtained in a previous μSR study²³. While the Néel temperatures we find are in good agreement with the data of Sugiyama *et al.*²³, there are also substantial differences. First, they obtained much smaller volume fractions of the magnetically ordered phase (about 20% in their polycrystalline $\text{Na}_{0.75}\text{CoO}_2$ sample and 50% in their $\text{Na}_{0.9}\text{CoO}_2$ single crystal). This suggests that their samples might have been less homogeneous, possibly due to an inhomogeneous distribution of Na. Another important difference may exist concerning the intercalation of water, which is known to occur rather rapidly under moist conditions, especially for powder samples. Secondly, the magnitude and number of the deduced muon spin precession frequencies are also rather different. In their polycrystalline samples, they also observe three muon frequencies, at about 3.3, 2.6 and 2.1 MHz. However, their relative amplitudes are different from those observed in our crystals, so that, for instance, the largest contribution comes from the highest-frequency mode. In their single-crystal sample, Sugiyama *et al.* observe only one frequency, though there is some evidence for at least one additional frequency²³.

This leaves us with the important question of whether the different local magnetic fields are a consequence of different crystallographic muon stopping sites, or whether they should be interpreted in terms of different magnetic environments. The latter may be caused

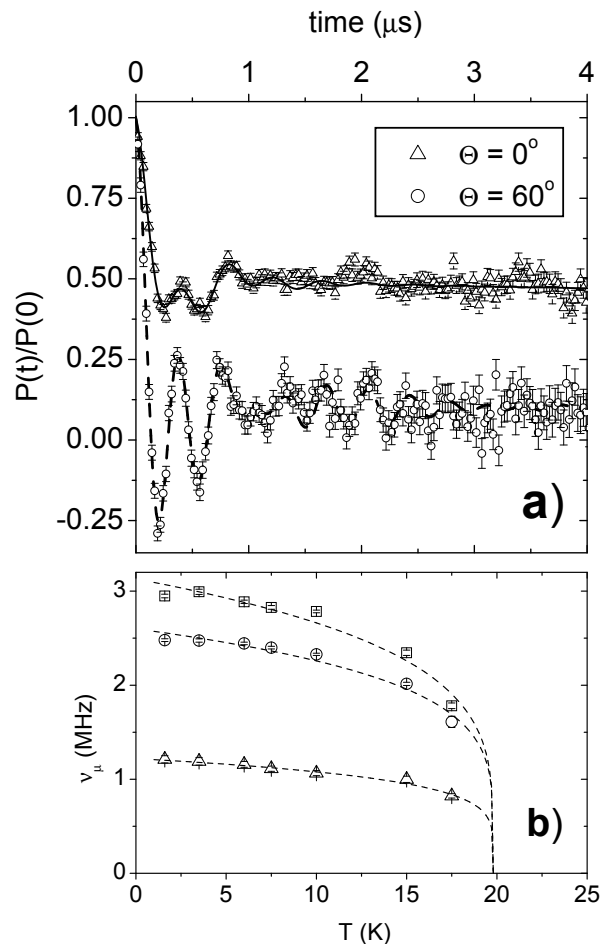


FIG. 3: a) Time dependence of the spin polarization of muons implanted in a $\text{Na}_{0.82}\text{CoO}_2$ crystal in zero field at $T = 7.5$ K. Θ is the angle subtended by the initial spin polarization and the crystallographic c -axis. The lines are the results of fits described in the text. b) Temperature dependence of the μSR frequencies extracted from the $P(t)$ spectra (panel a). The dashed lines are guides to the eye.

by commensurate magnetic order with a large unit cell, but could also arise from a macroscopically inhomogeneous magnetic state. As noted by Sugiyama *et al.*, the local fields experienced by the muons in different crystallographic muon sites should be mostly of dipolar origin. Potential muon stopping sites are close to the oxygen ions and near Na(1) or Na(2) vacancies. We performed a calculation of the dipolar fields for the case of Co moments directed along the c -axis and exhibiting A-type antiferromagnetic order. We find that the magnetic fields near the Na(1) and the Na(2) vacancies are vanishingly small. We therefore suggest that the muons are located primarily near the oxygen ions, forming a muoxyl bond, as in other oxide compounds including the cuprate high- T_c superconductors²². Assuming an ordered moment of $0.3 \mu_B$, we obtain a local magnetic field of about 2 MHz at the oxygen site.

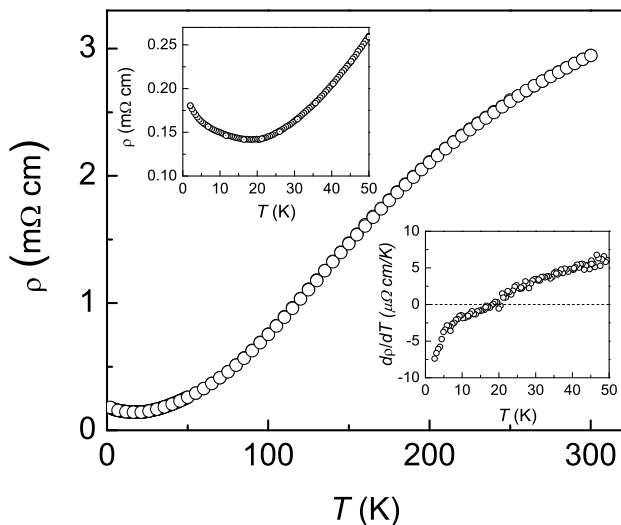


FIG. 4: In-plane resistivity of $\text{Na}_{0.82}\text{CoO}_2$. Insets: Low-temperature resistivity and its temperature derivative.

The three different muon-spin precession frequencies observed in the experiment could be due to the presence of a structural minority phase with a monoclinic distortion, as discussed in Ref. 13. However, if a minority phase were present in our sample, its Néel temperature would have to be very similar to that of the majority phase. This conclusion is based on the temperature dependence of the local magnetic fields, which is shown in Fig 3b. It is evident that all three local fields exhibit a similar T-dependence, i.e. they decrease towards the magnetic transition at 19.8 K evident in the magnetization and the specific heat data.

It is also possible that the three frequencies reflect a commensurate spin order in which the same local field is repeated in every third crystallographic unit cell. However, our data do not support an interpretation in terms of an incommensurate magnetic order²³, which should give rise to much larger depolarization rates and to a different form of the relaxation function. We have tried fitting with Bessel functions, but could not obtain a reasonable fit. Since μSR data provide only local information, it is not straightforward to deduce further information concerning the magnetic ordering pattern. Neutron scattering experiments will be required to settle this important issue.

Fig. 4 shows the in-plane resistivity measured on a rectangular crystal ($4 \times 3 \times 0.6 \text{ mm}^3$) with a four-point ac-technique ($\nu = 119 \text{ Hz}$). The resistivity is frequency-independent between 19 and 1000 Hz and exhibits metallic character for $T > T_N$, with a residual-resistivity ratio $\rho(300\text{K})/\rho(4.2\text{K}) \sim 20$. The temperature derivative of the resistivity changes sign at T_N (insets in Fig. 4). This is the behavior expected if a spin density wave opens a small gap at the Fermi surface.

In conclusion, the thermodynamic, transport, and μSR data reported here are consistent with an intrinsic, commensurate antiferromagnetic spin density wave transition at 19.8 K, but incompatible with incommensurate magnetic order²³. Our data may prove valuable in elucidating the origin of the large thermopower of Na_xCoO_2 and of the unconventional superconducting state in the closely related compound $\text{Na}_{0.35}\text{CoO}_2 \cdot 1.3 \text{ H}_2\text{O}$.

We acknowledge the technical support of A. Amato at the PSI, and E. Brücher and G. Siegle at the MPI.

- ¹ K. Takada, H. Sakurai, E. Takayama-Muromachi, F. Izumi, R. A. Dilanian, and T. Sasaki, *Nature* **422**, 53 (2003).
- ² J. W. Lynn, Q. Huang, C. M. Brown, V. L. Miller, M. L. Foo, R. E. Schaak, C. Y. Jones, E. A. Mackey, and R. J. Cava, *cond-mat/0307263*.
- ³ J. D. Jorgensen, M. Avdeev, D. G. Hinks, J. C. Burley, and S. Short, *cond-mat/0307627*.
- ⁴ D. J. Singh, *Phys. Rev. B* **61**, 13397 (2000); *ibid.* **68**, 020503(R) (2003).
- ⁵ W. Koshibae, K. Tsutsui, and S. Maekawa, *Phys. Rev. B* **62**, 6869 (2000); W. Koshibae and S. Maekawa, *cond-mat/0306696*.
- ⁶ C. Honerkamp, *Phys. Rev. B* **68**, 104508 (2003).
- ⁷ M. Renner and W. Brenig, *cond-mat/0310244*.
- ⁸ T. Waki, C. Michioka, M. Kato, K. Yoshimura, K. Takada, H. Sakurai, E. Takayama-Muromachi, and T. Sasaki, *cond-mat/0306036*.
- ⁹ T. Fujimoto, G.-Q. Zheng, Y. Kitaoka, R.L. Meng, L. Cmaidalka, and C.W. Chu, *cond-mat/0307127*.
- ¹⁰ G. Baskaran, *Phys. Rev. Lett.* **91**, 097003 (2003).
- ¹¹ Y. Tanaka, Y. Yanase, and M. Ogata, *cond-mat/0311266*.
- ¹² O.I. Motrunich and P.A. Lee, *cond-mat/0310387*.
- ¹³ C. Fouassier, G. Matejka, J. M. Reau, and P. Hagenmuller, *Jour. Sol. State Chem.* **6**, 532 (1973).
- ¹⁴ M. Jansen and R. Hoppe, *Z. Anorg. Allg. Chemie* **408**, 104 (1974).
- ¹⁵ R.J. Balsys and R.L. Davis, *Sol. State Ionics* **93**, 279 (1996).
- ¹⁶ T. Tanaka, S. Nakamura, and S. Iida, *Jpn. J. Appl. Phys.* **33**, L581 (1994).
- ¹⁷ Y. Wang, N. S. Rogado, R. J. Cava, and N. P. Ong, *Nature* **423**, 425 (2003); *cond-mat/0305455*.
- ¹⁸ I. Terasaki, Y. Sasago, and K. Uchinokura, *Phys. Rev. B* **56**, R12685 (1997).
- ¹⁹ T. Motohashi, E. Naujalis, R. Ueda, K. Isawa, M. Karpinen, and H. Yamauchi, *Appl. Phys. Lett.* **79**, 1480 (2001).
- ²⁰ D. P. Chen, H. C. Chen, A. Maljuka, A. Kulakov, H. Zhang, and C. T. Lin (unpublished).
- ²¹ P. Lemmens, V. Gnezdilov, N.N. Kovaleva, K.Y. Choi, H. Sakurai, E. Takayama-Muromachi, K. Takada, T. Sasaki, F.C. Chou, C.T. Lin, and B. Keimer, *J. Phys.: Cond. Mat.*, in press.

- ²² M. Weber, P. Birrer, F.N. Gygax, B. Hitti, E. Lippelt, H. Maletta, and A. Schenck, *Hyperfine Interact.* **63**, 207 (1990); N. Nishida and H. Miyatake, *ibid.* **63**, 183 (1990).
- ²³ J. Sugiyama, H. Itahara, J. H. Brewer, E. J. Ansaldo, T. Motohashi, M. Karppinen, and H. Yamauchi, *Phys. Rev. B* **67**, 214420 (2003); J. Sugiyama, J. H. Brewer, E. J. Ansaldo, B. Hitti, M. Mikami, and Y. M. T. Sasaki, *cond-mat/0310637*.